Published in final edited form as:
Anal Chem. 2013 June 18; 85(12): 5810–5818. doi:10.1021/ac400486u.

Impact of TiO_2 Nanoparticles on Growth, Biofilm Formation, and Flavin Secretion in *Shewanella oneidensis*

Melissa A. Maurer-Jones, **Ian L. Gunsolus**, **Ben M. Meyer**, **Cole J. Christenson**, and **Christy L. Haynes***
Department of Chemistry, University of Minnesota, 207 Pleasant St SE, Minneapolis, MN 55455

Abstract

Understanding of nanoparticle impacts on critical bacteria functions allows us to gain a mechanistic understanding of toxicity and guides us towards design rules for creating safe nanomaterials. Herein and using analytical techniques, biofilm formation, a general bacteria function, and riboflavin secretion, a species-specific function, were monitored in *Shewanella oneidensis*, a metal reducing bacterium, following exposure to a variety of TiO_2 nanoparticle types (synthesized, Aeroxide P25, and T-Eco). TEM images show that dosed nanoparticles are in close proximity to the bacteria but they are not internalized. Using quartz crystal microbalance (QCM), it was revealed that *S. oneidensis* biofilm formation is slowed in the presence of nanoparticles. Though *S. oneidensis* grows more slowly in the presence of TiO_2 nanoparticles, riboflavin secretion, a function related to the *S. oneidensis* metal reducing capacity, was increased significantly in a nanoparticle dose-dependent manner. Both changes in biofilm formation and riboflavin secretion are supported by changes in gene expression in nanoparticle-exposed *S. oneidensis*. This broad study of bacterial nanotoxicity, including use of sensitive analytical tools for functional assessments of biofilm formation, riboflavin secretion, and gene expression has implications for total ecosystem health as the use of engineered nanoparticles grows.

Keywords

titanium dioxide; nanoparticle; toxicity; quartz crystal microbalance; high performance liquid chromatography

Introduction

While nanoscale particles occur naturally and have been used intentionally for centuries, release of engineered nanoparticles into the environment via direct application (e.g. pesticides), waste water effluent and sludge, and product degradation, among other routes, is of concern due to the increasing production and use of these materials and their novel physical and chemical properties. Therefore, it has become increasingly important to characterize the fate, transformation, and toxicity of engineered nanoparticles in ecological systems. The work presented herein focuses on toxicity of titanium dioxide (TiO_2) nanoparticles, chosen due to their high commercial production rate; global production was 5000 tons in 2010[1] and is projected to increase to 2.5 million tons by 2025.[2] TiO_2

*chaynes@umn.edu.

Supporting Information
Nanoparticle characterization, viability assay methods and results, QCM drift, EPS characterization, sample preparation for TEM uptake analysis, ROS quantification and gene expression. This material is available free of charge via the Internet at http://pubs.acs.org.

nanoparticles are manufactured in a variety of forms, the most common being E171 (food additive),[1] T-Eco (sunscreens),[3] and Evonik Aeroxide® P25 (National Institute of Standards and Technology (NIST) established standard for TiO_2 nanoparticles).

Released engineered nanoparticles will potentially impact organisms on all levels of the food chain, but the most widespread consequences will result from impacts exerted on low trophic level organisms like bacteria, which play critical roles in the ecosystem. A mechanistic understanding of nanoparticle-induced bacterial toxicity has implications for understanding ecosystem health in general. *Shewanella oneidensis* MR-1 provides an excellent model system for understanding nanotoxicity as these bacteria are distributed world-wide in a variety of environments and are important for geochemical nutrient cycling.[4] Additionally, this bacterium has also recently been utilized in nanotoxicity studies as an environmentally relevant model, facilitating comparison of various nanomaterials.[5–6] Because *S. oneidensis* is an aquatic organism, there is a high likelihood that these bacteria will interact with nanoparticles entering the environment via the previously described routes.

Much of the work to date studying the bacterial toxicity of engineered nanoparticles has focused mainly on changes in viability and/or growth,[7–9] but elucidation of toxicity mechanisms requires assessment of cell function changes as well. Toward understanding the nature of nanoparticle/bacteria interactions, some strategies that have been employed thus far include study of nanoparticle uptake/association and post-exposure bacterial morphology,[10] membrane integrity and properties,[10–12] and oxidative stress.[10], [13] While characterizing the nature of nanoparticle-bacteria interaction is an area of increasing research, critical gaps remain in the understanding of bacterial function following nanoparticle interaction. Using analytical methodology to study nanoparticle toxicity to cellular function could enable a mechanistic understanding of the nanoparticle interaction; few strategies or methods have been employed for achieving such understanding, and thus, that is the aim of this work.

More specifically to address these gaps, we examine the effects of nanoparticle exposure on both a general bacterial function (biofilm formation) and a *S. oneidensis*-specific function (flavin secretion) using the sensitive analytical tools of quartz crystal microbalance (QCM) and high performance liquid chromatography (HPLC), respectively. Biofilms are composed of microorganisms embedded within a self-produced biopolymer matrix, and formation of these biofilms is a critical function for bacteria. Many of the important environmental functions performed by bacteria, including organic material production and degradation, toxic material degradation, and biogeochemical cycling of biogenic elements like nitrogen, oxygen, and phosphorous require cooperative metabolic functioning, as occurs in biofilms.[14] Biofilms serve a range of functions, both beneficial and detrimental to humans, which include acting as a food source for aquatic invertebrates, removing organic matter during sewage treatment, and biofouling. For *S. oneidensis*, formation of biofilms is important for their interaction with metals and metal oxides.[15] Beyond their importance to bacterial function, biofilms represent the most common arrangement of bacteria in the environment, and so studying the impact of nanoparticles on biofilm formation allows generalizable understanding of nanoparticle toxicity.

The main function of *S. oneidensis* in the geochemical cycle is as a metal reducer, a function which is performed by the secretion of electron shuttling molecules. More specifically, *S. oneidensis* secretes flavin mononucleotide from the periplasmic space, which is readily converted into riboflavin, and these are extracellularly reduced using electrons donated by organic carbon oxidation within the cell.[4] This function serves both to transform metals and as a method of respiration for *S. oneidensis* when oxygen content is limited.

Herein, we aim to establish new tools for nanotoxicity studies and more specifically, to understand the mechanism of toxicity of TiO_2 nanoparticles in a variety of forms (synthesized, Aeroxide P25, and T-Eco) on *S. oneidensis* by characterizing the nanoparticle impact on the generalizable function of biofilm formation and the species-specific function of metal reduction. QCM will be used to monitor biofilm formation and growth, which has been used previously in the study of bacterial biofilms,[16–18] and HPLC will be used to analyze riboflavin secretion from *S. oneidensis* suspensions. We hypothesize that increase or decreases in biofilm formation will correlate directly with increases and decreases in the riboflavin secretion. These assessments of functional changes as a result of TiO_2 nanoparticle exposure, complemented by gene expression studies, reveal new insights regarding the outcome of nanoparticle-bacteria interactions.

Experimental Section

Nanoparticles

Three types of TiO_2 nanoparticles were utilized in this study: acid-catalyzed TiO_2 nanoparticles synthesized in house (as-syn), Evonik Aeroxide® Degussa P25 (P25 - The Cary Company, Addison, IL) and Eusolex® T-Eco (T-Eco - EMD Chemicals Inc, Gibbstown, NJ). As-syn nanoparticles were synthesized and characterized as previously described,[19] and both commercial nanoparticles' (P25 and T-Eco) size and crystallinity have been characterized within the literature.[3, 20]

Beyond previous characterization, the hydrodynamic size, stability, and ζ-potential of 25 μg/ml nanoparticle suspensions in water and LB broth, bacterial growth broth, was examined using Brookhaven Instruments Corporation dynamic light scattering (DLS) and ZetaPALS Zeta Potential Analyzer (Holtsville, NY). Additionally, transmission electron microscopy (TEM) images were taken on a JEOL 1200 EXII (JEOL, Tokyo, Japan) at 80 kV.

Bacteria Culture and Nanoparticle Exposure

Shewanella oneidensis MR-1 stock was generously gifted from the lab of Jeff Gralnick at the University of Minnesota. The following method was employed to culture bacteria that were subsequently used in nanoparticle toxicity experiments. All bacteria culture and nanotoxicity experiments were performed in LB broth (BD Difco™, BD Diagnostics, Franklin Lakes, NJ) or agar (BD Difco™) plates with LB broth nutrients. *S. oneidensis*, stored at −80 °C, were inoculated onto a LB broth agar plate and incubated at 30 °C for 18–24 h, or until visible colony formation. Colonies were transferred to LB broth in sterile culture tubes with 1 colony placed in 5 mL of LB broth and allowed to come to stationary phase (~18–24 h). At this point, the bacteria were used for toxicity assessments and will herein be referred to as bacterial suspension. Typically, the bacterial suspension was at a cell density of 10^9 cells/ml, as measured by the OD at 600 nm where 1 absorbance unit equals 10^9 cells/mL. Nanoparticle exposures were conducted on the bacterial suspension in a range of 1–100 μg/ml TiO_2 nanoparticles from a suspension of nanoparticles in LB broth under ambient laboratory light. These concentrations were chosen as they fall within the range of predicted environmental concentrations for the release of TiO_2 from waste water effluent.[21]

Growth

To determine the impact of nanoparticles on bacterial growth, the optical density of bacteria was monitored over time to assess nanoparticle impact on growth rates. Cells from the bacterial suspension were diluted to 10^7 cells/ml and exposed to 0, 1, 5, 10, 25, or 100 μg/mL of either as-syn, P25, or T-Eco, and measurements of OD at λ=600 nm were periodically recorded with a Spectronic 20D (Milton Roy Company, Ivyland, PA), with samples replaced onto the shaking incubator when data were not being collected. The

exponential phase of growth was determined by manual inspection of each curve, and the growth rate, in generations/h, was determined using Equation 1, based on the classic binary fission model.

$$\text{growth rate}=\frac{\log OD_2 - \log OD_1}{0.301 \times (t_2 - t_1)} \quad \text{Equation 1}$$

Biofilm Assessment with QCM

QCM experiments to assess biofilm formation and growth were performed on a Maxtek, Inficon R-QCM system with 1" gold contact crystals in a flow cell (Inficon, East Syracuse, NY). QCM enables measurement of biofilm growth based on the principles of the Sauerbrey equation ($\Delta m=-C\Delta f$), where changes in the resonant frequency (Δf) of a bacteria-exposed quartz crystal are proportional to changes in mass (Δm), accounting for a crystal sensitivity factor (C). The Sauerbrey equation, however, assumes the deposited mass is rigidly bound to the crystal surface such that no damping occurs; this is not true of bacteria cells attaching to the surface. In this case, the series resonance resistance, which can be measured separately from the resonant frequency, is proportional to damping of the crystal resonance and, therefore, to the viscoelastic properties of the material deposited. A decrease in the series resonance resistance indicates a decrease in density of the deposited material. Herein, QCM measurements were used to assess both the mass of biofilm deposited on the crystal and the viscoelastic properties of the biofilm based on changes in frequency and resistance, respectively.

In the experimental set-up, the system was held at 30 °C in an incubator, and measurements were made on two parallel crystals, control and nanoparticle exposure conditions, with samples introduced to the flow cell using peristaltic pumps (variable flow mini-pump, Fisher Scientific, Hampton, NH). Additionally, there was a constant flow throughout the experiment. For biofilm growth experiments, LB broth was introduced to the flow cell at 0.25 mL/min and the crystal was allowed to equilibrate for ~1 h. After which, aerated bacteria were introduced to the crystal for ~1 h at a flow rate of 0.25 mL/min to allow attachment. Flow was switched back to aerated broth (without bacteria) and the flow was increased to 0.75 mL/min. TiO_2 nanoparticles (25 μg/mL) were introduced either simultaneously with bacteria and/or with aerated broth.

HPLC Measurement of Riboflavin

Flavin secretion by *S.oneidensis*, important for heavy metal reduction function, was monitored by analyzing suspensions for riboflavin using HPLC, taking advantage of riboflavin's native fluorescence. Bacterial suspensions diluted to 10^8 cells/mL were exposed to 0–100 μg/mL as-syn or 25 μg/mL P25 or T-Eco TiO_2 nanoparticles for 24 h, and exposures were made in triplicate. A 1 mL sample was removed from each suspension and centrifuged for 15 minutes at 5000 g. Then, 200 μL of the supernatant was transferred to an amber HPLC vial with a 250 μL glass insert. HPLC analysis of riboflavin was performed on an Agilent 1200 HPLC fitted with a Zorbax Eclipse XDB-C_{18} 4.6 × 150 mm, 5 μm analytical column and Eclipse XDB-C_{18} 4.6 × 12.5 mm, 5 μm analytical guard column ahead of the fluorescence detector. Isocratic elution was performed using a 70:30 mixture of 20 mM citric acid buffer (pH 3.3):methanol as the mobile phase. The injection volume was 30 μL, flow rate was 1 mL/minute, and detection of riboflavin was achieved with excitation and emission wavelengths of 450 nm and 530 nm, respectively. The run time was 7.25 minutes, and riboflavin elution was achieved after approximately 6.5 minutes.

Extracellular Polymeric Substance Isolation and Characterization

Due to its importance in biofilms and to examine other secretion behaviors of *S. oneidensis*, the extracellular polymeric substance (EPS) was extracted and characterized for its sugar and protein content as previously described by Gong et al.[22] after 24 h exposure to varying concentrations of as-syn TiO_2 nanoparticles and 25 μg/mL P25 and T-Eco. Briefly, polysaccharides were reacted with phenol and sulfuric acid and proteins were reacted with Lowry's reagents and the products of these reactions, measured separately, were assessed spectrophotometrically (detailed method in supporting information).

Uptake Assessment with TEM

Determination of TiO_2 nanoparticle internalization or association with *S. oneidensis* was completed utilizing TEM with a modified method described previously[19] and described in detail in Supporting Information. Briefly, bacteria were cultured cultured with 25 μg/mL as-syn TiO_2 at varying lengths of exposure, fixed with a solution of 2.5% glutaraldehyde and 1% osmium tetraoxide, and embedded in Epon resin (Polybed 812). Samples were sectioned, stained with uranyl acetate and lead citrate (Sigma-Aldrich, St. Louis, MO) and imaged on JEOL 1200 EXII TEM at 60 kV.

Reactive Oxygen Species Quantification

Intracellular reactive oxygen species (ROS) were monitored using two different assays: DCFDA and APF (Life Technologies, Grand Island, NY). DCFDA is generally considered to react with most ROS molecules, and APF reacts more specifically with hydroxyl radical. The bacterial suspension was pelleted (1500×g for 10 min), and the supernatant was decanted. Cells were resuspended in LB broth with either 10 μM DCFDA or 5 μM APF for one hour to allow cell uptake of fluorescent probe molecule. The bacterial suspension was again centrifuged (1500×g for 10 min), and cells were washed 3 times with LB broth to remove extracellular DCFDA or APF. Bacteria were exposed to as-syn TiO_2 nanoparticles in triplicate as described above in a range of 1–100 μg/mL, with no nanoparticles as a negative control and 10 μM sodium hypochlorite as a positive control. Periodically, a 250 μL samples was taken from each condition, placed in a 96 well plate, and the fluorescence intensity was measured at $\lambda_{excitation}$ = 485/20 nm and $\lambda_{emission}$ = 528/20 nm for both assays.

Quantitative Reverse Transcription Polymerase Chain Reaction (qRT-PCR)

qRT-PCR was performed on samples of *S. oneidensis* exposed to 0–100 μg/mL as-syn TiO_2 after varied amounts of time and/or 25 μg/mL P25 or T-Eco after a 24 h exposure (experiments performed in 3 biological and 2 technical replicates). Primers were ordered through the BioMedical Genomics Center Oligonucleotide & Peptide Synthesis service using Integrated DNA Technologies (IDT) (Coralville, IA). Assay design was prepared using the Roche Universal Probe Library (UPL) technology. To validate the primer probe sets, a five point 1:5 dilution series of the cDNA sample was carried out. Total RNA was isolated using RNAzol® RT (Sigma Aldrich, St. Louis, MO) following manufacturer protocols. Total RNA samples were synthesized to first-strand cDNA using SuperScript® II RT from Invitrogen (Life Technologies, Grand Island, NY). Quantitative PCR was performed on the ABI 7900 HT (Life Technologies, Grand Island, NY) using 3 μLs of cDNA in duplicate. A working cocktail was made by adding 10 μM forward primer (IDT), 10 μM reverse primer (IDT), 10 μM probe (UPL), and 2.22X homebrew master mix. 3 μLs of cocktail was added to 3 μL aliquots of cDNA samples and amplified by the following parameters: 2 min activation at 60 °C and a 5 minute denaturation at 95 °C, followed by 45 cycles of 10 seconds at 95 °C and 1 minute at 60 °C.

Data analysis was performed using the Pfaffl method in which the amount of the target gene was normalized to a reference gene, *gyrB*, and compared to control samples. 1-way ANOVA analysis was performed to determine significant changes in gene expression levels.

Results and Discussion

Nanoparticle Characterization

Three types of TiO_2 nanoparticles were utilized in this study, acid-catalyzed TiO_2 nanoparticles synthesized in house (as-syn), Evonik Aeroxide® Degussa P25 (P25) and Eusolex® T-Eco (T-Eco). As-syn nanoparticles were synthesized and characterized as previously described,[19] and were chosen because of the controlled crystallinity and surface chemistry that in-house synthesis affords. Two commercially available TiO_2 nanoparticles, P25 and T-Eco, were chosen because P25 is often used as a "model" TiO_2 nanoparticle in toxicity studies[23] and T-Eco has been shown to be most similar to nanoparticles present in cosmetics, including sunscreens.[3] Both commercial nanoparticles' size and crystallinity have been characterized within the literature.[3, 20] Stability and ζ-potential of synthesized nanoparticles were measured in water and Luria-Bertani (LB) broth, the bacterial growth broth used in toxicity experiments, to better understand the aggregation state of the nanoparticles during these experiments. It should be noted that aggregation was not controlled within these studies as aggregation is not systematically controlled in the environment, though future work aimed at understanding natural organic matter-mediated aggregation will be performed. These data, along with data on size and crystallinity that has been previously reported,[3, 19–20] are summarized in supporting information (Figure S1). Generally, all three TiO_2 materials aggregate over 24 h, though T-Eco aggregated significantly less than as-syn and P25, possibly due to the T-Eco surface being coated with a thin layer of SiO_2. All nanoparticles in LB broth aggregated less than in water, likely because LB contains many biological macromolecules that can adsorb onto the surface and prevent aggregation.

TiO_2 Nanoparticles' Impact on Viability and Growth

To begin toxicity studies, cell survival upon nanoparticle exposure was measured using differential fluorescent staining of live and dead cells to yield a live/dead ratio measure of viability (See Supporting Information for methods and results). Evaluating the viability of *S. oneidensis* after exposure to TiO_2 nanoparticles for various exposure times revealed no significant change in cell survival with increasing concentrations of as-syn TiO_2 over 24 h or with the other two nanoparticle sample types (Figure S2), consistent with previous assessments of TiO_2 bacterial toxicity.[24–25] There was some change in the ratio of live to dead bacteria over time (Figure S2B), but this was due to growth of bacteria within the experiment, and the same pattern of live/dead ratio changes were observed in all nanoparticle and control experiments.

While viability was not altered in the presence of nanoparticles, TiO_2 caused a dose-dependent decrease in the growth rate of *S. oneidensis* (Figure 1), as determined by optical density measurements. By plotting the absorbance over time on a log scale, the exponential phase of growth was observed, and the growth or doubling rate was calculated using Equation 1 and quantified in the inset of Figure 1A. It was noted that initially, scattering from the nanoparticles contributed to the optical density measurements. To confirm that we were observing changes as the result of slowed growth, the optical density minus the initial optical density, which ranged in absorbance values from 0.03–0.3 absorbance units, was plotted, and differences in growth are still apparent (Figure 1B). Performing statistical analysis of linear regression fits of the data presented in Figure 1B (lines not shown) reveals that the rates of growth of all nanoparticle-exposed bacteria are significantly different than

that of the control ($p<0.01$). A similar decrease in doubling rate was observed for all three nanoparticles, an indication that the nanoparticles were having a similar impact on bacterial growth. This trend may be a result of non-specific adsorption of broth components onto the nanoparticle surface. Altered bacterial growth rate in the presence of TiO_2 nanoparticles has not been previously reported in *S. oneidensis* or other bacterial species. Decreases in bacterial growth rate can be caused by changes or decreases in the available nutrients or available organic carbon (AOC).[26] Stability of the nanoparticles in LB broth (data in Figure S1) suggests adsorption of components from LB broth onto the nanoparticle, an adsorption phenomena that is widely reported in the literature with proteins,[27] natural organic matter,[28] and other biomacromoleules.[29] One could imagine, therefore, that the decrease in growth is caused by nutrient adsorption onto the nanoparticle surface causing a decrease in the AOC that, in turn, would decrease the growth rate. Future work aimed at studying the influence of nanoparticles on the broth components and natural organic matter will address these observations.

Changes in Bacterial Functions

Biofilm Formation and Growth—Moving beyond viability and growth, a functional assessment of *S. oneidensis* was performed examining both a general bacteria and species-specific function. As mentioned previously, biofilm formation is a common function of bacteria of varied species and plays an important role in the way bacteria react to their surroundings,[30] with or without nanoparticles in this case. continuous monitoring of frequency and resistance, which relates dissipation, was performed over the course of the experiment to better understand the change in mass on the crystal and viscoelastic properties of the biofilm, respectively. First, a comparison between control and 25 μg/mL as-syn TiO_2 nanoparticle-exposed cells was examined, where nanoparticles were introduced to the bacteria during the attachment phase to the QCM crystal and throughout biofilm growth (results shown in Figure 2). Figure 2A details the change in frequency of the parallel crystals. A notable characteristic of both the control and TiO_2-exposed bacteria is that the change in frequency is not linear. For control cells, an initial rapid decrease in frequency is observed as compared to the TiO_2 condition, indicating the addition of mass to the crystal, followed by a 'lag' and then further decrease in frequency. This pattern indicates that there is an initial attachment of bacteria to the crystal with a delay before the biofilm begins to grow. This pattern is in contrast to the results of biofilm formation among TiO_2-exposed bacteria, where there is a steady, but less steep change in frequency, with growth increasing after 12 h. We confirmed that the change in frequency was the result of biofilm growth or the combination of cell attachment/growth and TiO_2 deposition as opposed to TiO_2 nanoparticle sedimentation alone by a similar experiment excluding bacteria (Supporting Information Figure S3). This experiment showed there was drift within the system where the change in frequency became more negative, possibly due to adsorption of molecules from LB broth, but not deposition of TiO_2, and the drift was, at most, half that of the bacteria experiments. In general, QCM revealed that TiO_2 nanoparticle-exposed bacteria yield a slower change in frequency (Figure 2A) indicating a slower biofilm growth, which is consistent with the decrease in growth rate demonstrated with optical methods above. Additionally, we considered the viscoelastic differences between control and nanoparticle-exposed biofilms, but there was no appreciable difference in the change in resistance of the biofilm with and without nanoparticle exposure (Figure 2B). Another way to examine this is to plot the change in resistance divided by the change in frequency, and for both the control and TiO_2-exposed cells, there is no difference (graph not shown), indicating that the quality of formed biofilms is not compromised by the presence of nanoparticles.

To elucidate whether the changes in biofilm growth were the result of changes in cell attachment, as opposed to simply the slowing of the rate of growth, we exposed cells to

TiO_2 nanoparticles, of all three types, only during attachment and continued to monitor growth after nanoparticles were no longer present. Results varied (Figure 3), where as-syn TiO_2 nanoparticles seemed to promote adhesion, P25 inhibited adhesion, and T-Eco had no effect. However, the variations during attachment were small, and these differences could be due to the variations within cell populations. While it cannot be concluded that bacterial attachment is unaffected by the presence of TiO_2 nanoparticles, any nanoparticle-based impact appears to be small.

Riboflavin Secretion—Another critical, species-specific function of *S. oneidensis* is metal reduction, where electron transfer occurs through the secreted molecule flavin mononucleotide (FMN).[31] FMN is converted to riboflavin, which was the molecule of interest in this study because FMN transforms to riboflavin even without the presence of a metal electron acceptor. Since *S. oneidensis* is responsible for metal reduction, one would predict stimulation of riboflavin secretion upon nanoparticle exposure; however, the energy required to reduce titanium (IV) likely exceeds the capability of the flavin reducing mechanism. Accordingly, we hypothesized that riboflavin secretion would decrease with nanoparticle exposure and correlate with the decrease in growth, which relates to a study correlating increases in *S. oneidensis* growth with flavin secretion.[32] After exposure to varying concentrations (0–100 μg/mL) and type of TiO_2 nanoparticles for 24 h, the extracellular riboflavin content was examined using HPLC, detecting the native fluorescence of riboflavin. Unexpectedly, extracellular riboflavin increased as a function of nanoparticle concentration (Figure 4A), though no differences were apparent upon comparing the different TiO_2 materials (Figure 4B). While there lacks literature precedent of *S. oneidensis* stress responses, this may be an indication that *S. oneidensis* flavin secretion is activated as a response to a system stressor.

To examine if other secretion processes were affected by the presence of TiO_2, isolation and characterization of EPS for the sugar and protein content was performed as it relates both to secretion events and biofilm formation. That is, EPS is commonly considered to be the structural support for biofilms and is a mixture of macromolecules including secreted proteins and polysaccharides. Hessler et al. recently noted that EPS has a role in mitigating TiO_2 nanoparticle toxicity in *Pseudomonas aeruginosa* as measured by the Live/Dead Baclight™ assay.[24] In quantifying the protein and polysaccharide content of TiO_2 nanoparticle-exposed *S. oneidensis* (methods described in supporting information), no change in the EPS was observed over the range of concentrations (1–100 μg/mL) or for the varied nanoparticle type after 24 h exposure (Supporting Information Figure S4). This indicates that growth and flavin secretion do not correlate to EPS production but could explain why changes in viability were not observed.

Processes that Influence Changes in Cell Functions

Uptake and Oxidative Stress—Toward a mechanistic understanding of the changes in function that were observed in *S. oneidensis* after TiO_2 nanoparticle exposure, we examined nanoparticle uptake or association, oxidative stress, and gene expression. Using TEM, we observed that TiO_2 nanoparticles are not internalized and do not appear to be membrane bound, though they are associated with the cells in some way as they are not washed off during rinse steps (Figure 5). This association was observed even after just a 2 h exposure.

Oxidative stress, or the production of ROS, is commonly considered to contribute to the mechanism of TiO_2 nanoparticle toxicity[33] and therefore, may contribute to the toxicity response measured herein (i.e. decreased growth and increased riboflavin secretion). Intracellular ROS was measured by first loading *S. oneidensis* with 2',7'-dichlorodihydrofluorescein diacetate (DCFDA) and aminophenyl fluorescein (APF) probe

molecules, followed by exposure to varying concentrations of TiO_2 nanoparticles (0–100 μg/mL) for varying amounts of time (results in Supporting Information). Over time, the intracellular ROS increases for all conditions, but over the first 6 h, there is no significant difference between control and nanoparticle-exposed cells. By 24 h, a difference in ROS production is observed, but there is no trend with nanoparticle concentration, and repeated experiments across 9 biological replicates reveal that the observed differences are inconsistent (Figure S5). A similar response is seen with both the DCFDA and APF assays (data not shown). These results indicate that ROS levels are not correlated with measured changes in growth and riboflavin production, and observed ROS may simply be associated with normal biological processes or functions. It is proposed that UV light exposure could modulate the intracellular ROS levels[34] but preliminary experiments did not reveal such modulations and will be the subject of future work.

Gene Expression—Moving beyond uptake and oxidative stress, we examined the impact of TiO_2 nanoparticles on gene expression, which may reveal the source for the varied growth, biofilm formation and flavin secretion. Genes encoding for a variety of functions were explored using quantitative reverse transcription-polymerase chain reaction (qRT-PCR) after a 24 h exposure to varied concentrations of as-syn TiO_2 (Figure 6 and Supporting Information Table S1) and 25 μg/mL P25 and T-Eco. Interestingly, in all genes explored, P25 and T-Eco imparted no significant change in gene expression as compared to the control (data not shown) whereas as-syn nanoparticles induced some changes. Since no other toxicity assessments demonstrated a different response based on the material, it is unclear what parameters would cause as-syn to induce varied gene expression from P25 and T-Eco, though it may be the result of a different surface crystallinity (P25 is 25% rutile) and surface material (T-Eco has SiO_2 at the surface). Further exploration of how the chemical interface influences gene expression will be an area of future work, as it is beyond the scope of this study.

Flavin secretion by *S. oneidensis* is the main method of electron transfer in their metal reducing function, and metal reduction occurs as the result of signaling that ends with the Mtr pathway.[35–36] Genes related to this pathway studied herein include *cymA*,[37–38] *ushA*,[31] *omcA*,[36] and *mtrA*.[35] While no significant trends are apparent for *cymA*, *mtrA*, and *ushA*, *omcA* shows significant ($p<0.05$) increase in gene expression after 24 h exposure to 10 μg/mL TiO_2 nanoparticles. While not significant, the other culture conditions are trending toward increased expression. *omcA* encodes for an outer membrane c-type cytochrome that plays a small role as a terminal reductase for metals and is also related to attachment of the cells to a solid surface.[36] Increased expression of this gene correlates with the increased riboflavin secretion by *S. oneidensis* over the 24 h exposure and also indicates that cell attachment as a biofilm may ultimately be affected, though this effect has not yet been observed. Other genes relating to biofilm formation and growth are the *mxdABCD* complex,[39–40] and the expression of each of these genes was quantified after 24 h nanoparticle exposure. Of these, both *mxdA* (Figure 6) and *mxdB* (Table S1) showed decreased expression as compared to the control. *mxdA* encodes for a diguanaylate cyclase protein and *mxdB* encodes for an inner membrane glycosyltransferase, both of which relate to cell attachment and synthesis of exopolymeric saccharides and to EPS.[39–40] These genes are essential for the three-dimensional growth of biofilms. Since these are both down regulated after exposure to most concentrations of nanoparticles, this may explain the decrease in growth of biofilm, as observed with QCM, because the syntheses of proteins for three dimensional growth are synthesized in lower amounts. However, the relationship of *mxdA* and *mxdB* to EPS would potentially indicate changes in the secretion profile that were not observed in the EPS characterization (Figure S4). It is possible that the EPS analysis is not sensitive enough to see these changes. Alternatively, the expression of these genes at 24 h may differ from the expression at early time points. That is, gene expression

may be initially stimulated upon TiO_2 nanoparticle exposure. This stimulation produces a level of protein that then causes a decrease in expression at the measured 24 h time point. The combination of the up-and down-regulation of gene expression ultimately yields a zero net balance to the content of the EPS.

Other genes of interest included *ftsK*, responsible for chromosome partitioning proteins that relate to growth,[41] and various stress response genes. These stress response genes include *sodB* and *gst*, which code for ROS response proteins superoxide dismutase B and glutathione transferase,[42] *pspB*, which codes for cytoplasmic membrane stress indicator phage shock protein,[43] *dnaN*, responsible for DNA polymerase protein, and *radA*, which encodes for DNA repair proteins. Of these, significant changes in gene expression were observed only for *sodB* and *pspB*. It is unsurprising to see no trend for *ftsK* expression because after 24 h, the bacterial culture has reached stationary phase, even in the presence of nanoparticles; therefore, the presence of chromosome partitioning proteins should be a steady state for all conditions. *pspB* expression levels (Table S1) were significantly higher for cells exposed to 25 μg/mL TiO_2 as compared to the control, indicating increased cytoplasmic membrane stress. In the case of *sodB*, there is a decreasing trend of *sodB* expression after 24 h exposure with lower nanoparticle concentrations, with a significant decrease at 10 μg/mL as-syn TiO_2 nanoparticles, though the expression is recovered at 25 and 100 μg/mL. This expression was unexpected because if oxidative stress had occurred, an increased expression would be expected. Again, the decrease may be the result of quantification of gene expression after 24 h exposure, and earlier time points may yield a different expression level. This is particularly true for oxidative stress, as typically oxidative stress effects are observed on short time scales due to the short lifetime of the ROS molecules.[44]

Given the rapid turnover of bacteria, gene expression at time-points earlier than 24 h was evaluated to see if changes induced earlier in the exposure period that are no longer detectable at 24 h may contribute to altered bacterial function. We took periodic samples of *S. oneidensis* exposed to 25 μg/mL as-syn TiO_2 nanoparticles and monitored expression of *omcA*, *mxdA*, *ftsK*, and *sodB* as these genes showed significant changes in expression after 24 h exposure that may be related to exposure time. As seen in Figure 7, *sodB* showed no significant trend over time as compared to the control, supporting the previous conclusion that oxidative stress does not appear to be the root of *S. oneidensis* growth and flavin secretion changes. The lack of change in *ftsK* as compared to the control indicates that this gene is not responsible for the changes in growth rate that have been observed, and further exploration of other candidate genes is needed. *omcA* showed an initial decrease in expression followed by increased expression at 3 h with an overall increased expression at 24 h. This trend in gene expression matches earlier riboflavin quantification experiments (data not shown) where minimal differences in riboflavin secretion is observed between the control and TiO_2-exposed bacteria, and it is only after prolonged exposure (24 h) that TiO_2 nanoparticles play a role in stimulating flavin secretion. For *mxdA*, an initial increase in expression is observed until 3 h, after which, expression is not different from that of the control. The initial burst (until 3h) followed by return to control level at 6 h and ultimate decrease in expression after 24 h may indicate that after there is a threshold level of protein available to the bacteria, the gene expression is depressed. This initial burst followed by decreased expression would explain why changes in EPS were not observed. In relationship to biofilm formation and growth, the lack of difference in gene expression after 1 h could explain why only minor differences in biofilm attachment were observed (Figure 3) but growth of the biofilms over time was depressed.

Conclusions

In summary, we demonstrated that, while minimal changes in viability were observed, significant changes in bacterial growth, biofilm growth and riboflavin secretion of *S. oneidensis* occurred after exposure to TiO_2 nanoparticles. These changes were not the result of oxidative stress, but the proximity of the nanoparticles caused altered gene expression that influenced the end-points measured in bacterial function assays (i.e., biofilm growth and riboflavin secretion). Though there were some minor toxicity differences among the three TiO_2 preparations considered herein, generally, each type of TiO_2 nanoparticle (i.e. as-syn vs. P25 vs. T-Eco) elicits similar functional changes within *S. oneidensis*, and the discrepancies and similarities are likely the result of surface structure and will be the subject of future work. This study indicates that TiO_2 nanoparticles are not lethal to *S. oneidensis*, but cause subtle changes to the bacterial function. The photocatalytic nature of TiO_2 nanoparticles may mean that UV light exposure will exacerbate these functional changes or make the nanoparticles lethal as previous studies have demonstrated.[45–46] Therefore, gaining an understanding of the functional changes within a species upon exposure to nanoparticles may be critical for understanding subtle or more drastic changes in ecosystem health.

Though the field of econanotoxicity is relatively new, this study presents an important approach to studying toxicity. That is, through a nuanced view of toxicity (i.e. functional assessment), a clear understanding of the nanoparticle impact is gained, and this yields beneficial information to inform nanoparticle design and mitigate any unintentional toxicity.

Supplementary Material

Refer to Web version on PubMed Central for supplementary material.

Acknowledgments

We acknowledge Jeff Gralnick of the University of Minnesota for his generous gift of *S. oneidensis* MR-1 and his help answering our questions. Additionally, we thank Gregory Gibson, an undergraduate researcher at the University of Minnesota, for his work developing the bacteria protocols and the BioMedical Genomic Center for their help in the qRT-PCR portion of this work. This research was financially supported by a grant from the National Science Foundation (CHE-1152931), an American Chemical Society Division of Analytical Chemistry and University of Minnesota Doctoral Dissertation Fellowship awarded to M.A.M-.J., NIH Biotechnology Training Grant awarded to I.L.G. and an University of Minnesota Undergraduate Research Opportunity Program fellowship awarded to C.J.C. Parts of this work were carried out in the Characterization Facility, University of Minnesota, which receives partial support from NSF through the MRSEC program.

REFERENCES

1. Weir A, Westerhoff P, Fabricius L, Hristovski K, von Goetz N. Environ. Sci. Technol. 2012; 46:2242–2250. [PubMed: 22260395]
2. Robichaud CO, Uyar AE, Darby MR, Zucker LG, Wiesner MR. Environ. Sci. Technol. 2009; 43:4227–4233. [PubMed: 19603627]
3. Lewicka Z, Benedetto A, Benoit D, Yu W, Fortner J, Colvin V. Journal of Nanoparticle Research. 2011; 13:3607–3617.
4. Hau HH, Gralnick JA. Annu. Rev. Microbiol. 2007; 61:237–258. [PubMed: 18035608]
5. Wu B, Huang R, Sahu M, Feng X, Biswas P, Tang YJ. Sci. Total Environ. 2010; 408:1755–1758. [PubMed: 19931887]
6. Wu B, Zhuang W-Q, Sahu M, Biswas P, Tang YJ. Sci. Total Environ. 2011; 409:4635–4639. [PubMed: 21855961]
7. Li K, Chen Y. J. Hazard. Mater. 2012; 209–210:264–270.

8. Xiu, Z-m; Zhang, Q-b; Puppala, HL.; Colvin, VL.; Alvarez, PJJ. Nano Lett. 2012; 12:4271–4275. [PubMed: 22765771]
9. Pelletier DA, Suresh AK, Holton GA, McKeown CK, Wang W, Gu B, Mortensen NP, Allison DP, Joy DC, Allison MR, Brown SD, Phelps TJ, Doktycz MJ. Appl. Environ. Microbiol. 2010; 76:7981–7989. [PubMed: 20952651]
10. Simon-Deckers, Al; Loo, S.; Mayne-Lahermite, M.; Herlin-Boime, N.; Menguy, N.; Reynaud, Cc; Gouget, B.; CarrieÌre, M. Environ. Sci. Technol. 2009; 43:8423–8429. [PubMed: 19924979]
11. Lyon DY, Alvarez PJJ. Environ. Sci. Technol. 2008; 42:8127–8132. [PubMed: 19031913]
12. Li M, Pokhrel S, Jin X, MaÌ^dler L, Damoiseaux R, Hoek EMV. Environ. Sci. Technol. 2011; 45:755–761. [PubMed: 21133426]
13. Lyon DY, Brunet L, Hinkal GW, Wiesner MR, Alvarez PJJ. Nano Lett. 2008; 8:1539–1543. [PubMed: 18410152]
14. Davey ME, O'Toole GA. Microbiol. Mol. Biol. Rev. 2000; 64:847–867. [PubMed: 11104821]
15. Marsili E, Baron DB, Shikhare ID, Coursolle D, Gralnick JA, Bond DR. Proc. Natl. Acad. Sci. U. S. A. 2008; 105:3968–3973. [PubMed: 18316736]
16. Nivens DE, Chambers JQ, Anderson TR, White DC. Anal. Chem. 1993; 65:65–69.
17. Schofield AL, Rudd TR, Martin DS, Fernig DG, Edwards C. Biosens. Bioelectron. 2007; 23:407–413. [PubMed: 17580113]
18. Reipa V, Almeida J, Cole KD. J. Microbiol. Methods. 2006; 66:449–459. [PubMed: 16580080]
19. Maurer-Jones MA, Lin Y-S, Haynes CL. ACS Nano. 2010; 4:3363–3373. [PubMed: 20481555]
20. Vasiliev PO, Faure B, Ng JBS, Bergström L. J. Colloid Interface Sci. 2008; 319:144–151. [PubMed: 18067910]
21. Gottschalk F, Scholz RW, Nowack B. Environmental Modelling and Software. 2010
22. Gong AS, Bolster CH, Benavides M, Walker SL. Environ. Eng. Sci. 2009; 26:1523–1532.
23. NIo. S. a. Technology. 2013 vol. January 2013.
24. Hessler CM, Wu M-Y, Xue Z, Choi H, Seo Y. Water Res. 2012; 46:4687–4696. [PubMed: 22789757]
25. Heinlaan M, Ivask A, Blinova I, Dubourguier H-C, Kahru A. Chemosphere. 2008; 71:1308–1316. [PubMed: 18194809]
26. TF T, Aquat RL. Microb. Ecol. 1997; 13:19–27.
27. Mahmoudi M, Lynch I, Ejtehadi MR, Monopoli MP, Bombelli FB, Laurent S. Chem. Rev. 2011; 111:5610–5637. [PubMed: 21688848]
28. Liu J, Legros S, Ma G, Veinot JGC, von der Kammer F, Hofmann T. Chemosphere. 2012; 87:918–924. [PubMed: 22349061]
29. Zhang S, Jiang Y, Chen C-S, Spurgin J, Schwehr KA, Quigg A, Chin W-C, Santschi PH. Environ. Sci. Technol. 2012; 46:8764–8772. [PubMed: 22834414]
30. Bandara H, Lam OLT, Jin LJ, Samaranayake L. Crit. Rev. Microbiol. 2012; 38:217–249. [PubMed: 22300377]
31. Covington ED, Gelbmann CB, Kotloski NJ, Gralnick JA. Mol. Microbiol. 2010; 78:519–532. [PubMed: 20807196]
32. von CH, Ogawa J, Shimizu S, Lloyd JR. Applied Environmental Microbiology. 2008; 74:615–623. [PubMed: 18065612]
33. Jiang G, Shen Z, Niu J, Bao Y, Chen J, He T. J. Environ. Monit. 2011; 13:42–48. [PubMed: 21127813]
34. Love SA, Maurer-Jones MA, Thompson JW, Lin YS, Haynes CL. Cooks RG, Yeung ES. Annual Review of Analytical Chemistry. 2012; 5:181–205. vol. 5.
35. Coursolle D, Gralnick JA. Frontiers in Microbiology. 2012; 3:56. [PubMed: 22363330]
36. Coursolle D, Baron DB, Bond DR, Gralnick JA. J. Bacteriol. 2010; 192:467–474. [PubMed: 19897659]
37. Myers CR, Myers JM. J. Bacteriol. 1997; 179:1143–1152. [PubMed: 9023196]
38. Marritt SJ, Lowe TG, Bye J, McMillan DGG, Shi L, Fredrickson J, Zachara J, Richardson DJ, Cheesman MR, Jeuken LJC, Butt JN. Biochem. J. 2012; 444:465–474. [PubMed: 22458729]

39. Thormann KM, Duttler S, Saville RM, Hyodo M, Shukla S, Hayakawa Y, Spormann AM. J. Bacteriol. 2006; 188:2681–2691. [PubMed: 16547056]
40. Saville RM, Dieckmann N, Spormann AM. FEMS Microbiol. Lett. 2010; 308:76–83. [PubMed: 20487019]
41. McLean JS, Pinchuk GE, Geydebrekht OV, Bilskis CL, Zakrajsek BA, Hill EA, Saffarini DA, Romine MF, Gorby YA, Fredrickson JK, Beliaev AS. Environ. Microbiol. 2008; 10:1861–1876. [PubMed: 18412550]
42. Thompson DK, Beliaev AS, Giometti CS, Tollaksen SL, Khare T, Lies DP, Nealson KH, Lim H, Yates J, Brandt CC, Tiedje JM, Zhou J. Appl. Environ. Microbiol. 2002; 68:881–892. [PubMed: 11823232]
43. Bencheikh-Latmani R, Williams SM, Haucke L, Criddle CS, Wu L, Zhou J, Tebo BM. Appl. Environ. Microbiol. 2005; 71:7453–7460. [PubMed: 16269787]
44. Lesser MP. Annu. Rev. Physiol. 2006; 68:253–278. [PubMed: 16460273]
45. Sadiq IM, Chandrasekaran N, Mukherjee A. Current Nanoscience. 2010; 6:381–387.
46. Dalai S, Pakrashi S, Kumar RSS, Chandrasekaran N, Mukherjee A. Toxicology Research. 2012; 1:116–130.

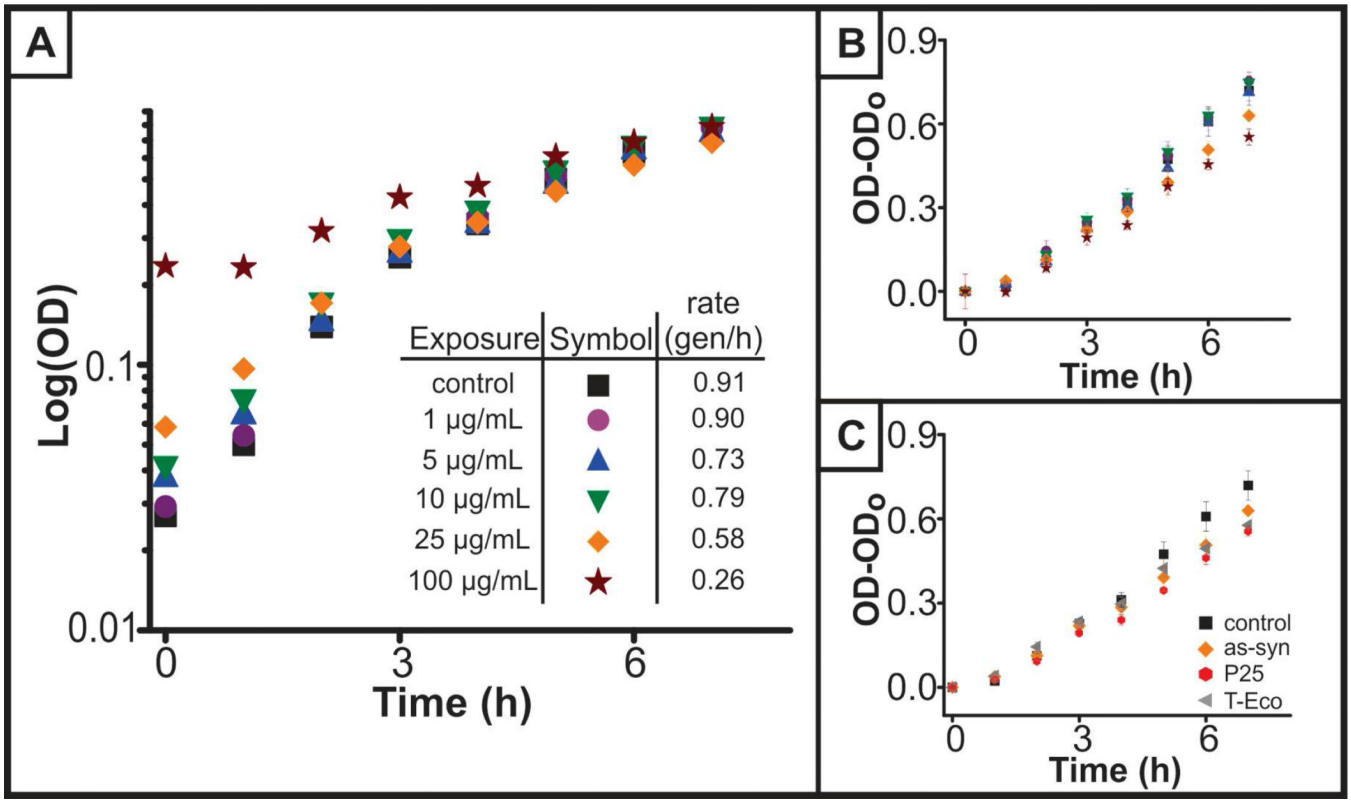

Figure 1.

Growth of *S. oneidensis* in the presence of TiO_2 nanoparticles. (A) Exponential phase of bacteria grown in the presence of varying concentrations of as-syn TiO_2 nanoparticles. Inset indicates growth rate of bacteria as determined by Equation 4.1. (B) Exponential phase of growth, with optical density at time = 0h subtracted to take into account scattering from as-syn nanoparticles. Statistical analysis of the linear regression of control and nanoparticle-exposed *S. oneidensis* revealed that all concentrations of nanoparticle-exposure regressions are statistically different than the control ($p<0.001$). (C) Comparison of the growth of *S. oneidensis* in the presence of 25 µg/mL as-syn, P25, or T-Eco nanoparticles.

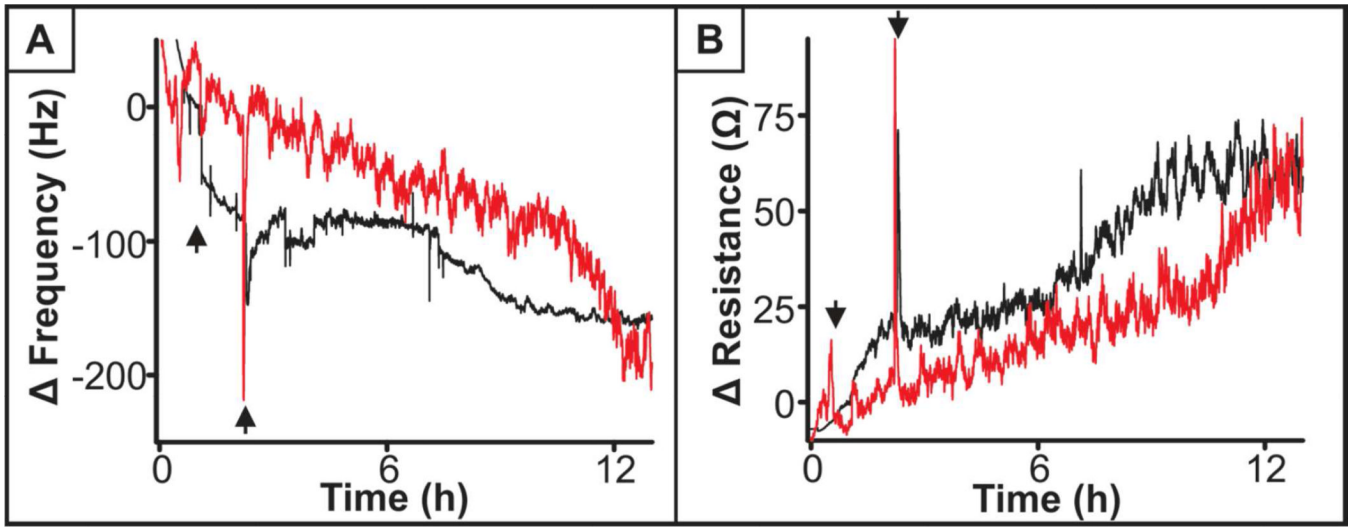

Figure 2.

QCM response to bacterial biofilm formation and growth without (black) and with (red) exposure to 25 μg/mL as-syn TiO_2 nanoparticles. (A) Changes in deposited mass as measured by the change in frequency and (B) the viscoelastic properties as measured by changes in quartz crystal resistance. Arrows indicate the window of time where *S. oneidensis* are introduced to the QCM flow cell. Outside of this time range, flow consisted of aerated LB broth without or with TiO_2.

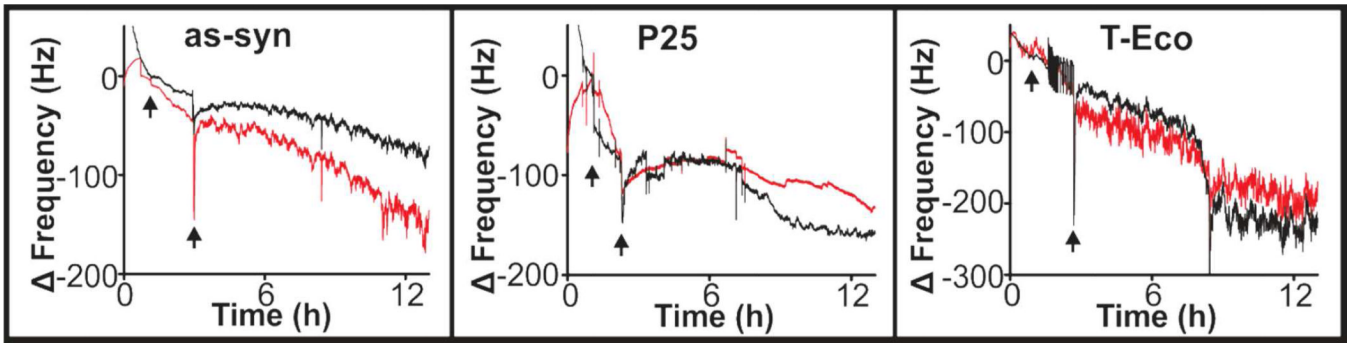

Figure 3.
QCM analysis of bacteria exposed to 25 μg/mL as-syn, P25, or T-Eco nanoparticles during bacterial attachment, indicated by the window of time between the arrows. Red = TiO_2 exposure and black = control (no nanoparticles) introduced in LB broth.

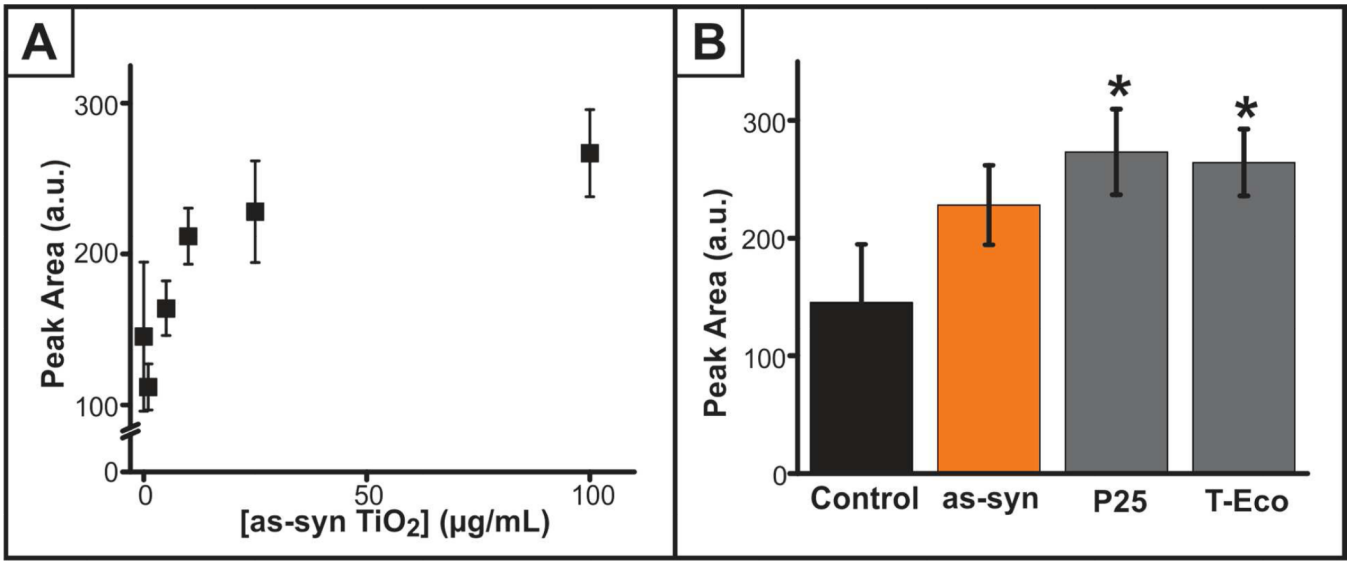

Figure 4.

Riboflavin secretion, as measured with HPLC, (A) is significantly increased ($p<0.05$) upon exposure to varying concentrations of as-syn TiO_2 nanoparticles for 24 h. (B) A comparison of riboflavin secretion upon exposure to 25 μg/mL as-syn, P25, and T-Eco (*$p<0.05$ as compared to the control).

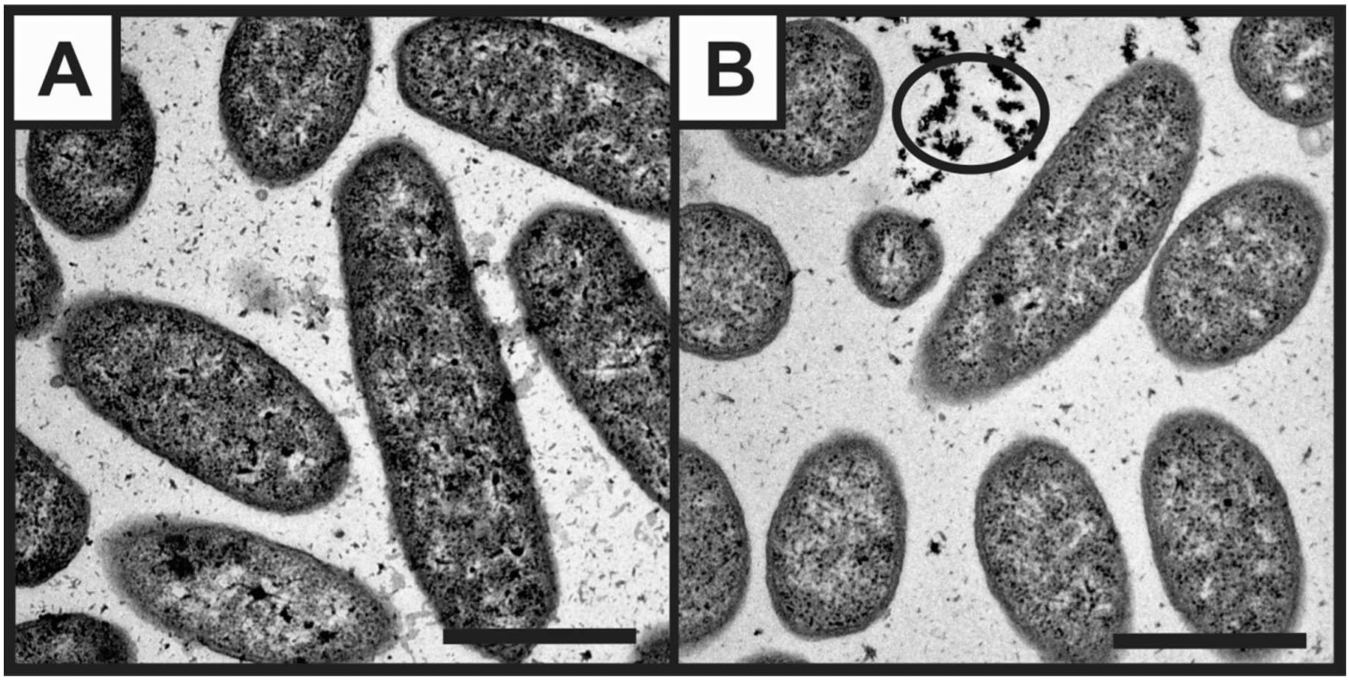

Figure 5.
TEM images of *S. oneidensis* after 6 h incubation (A) without or (B) with 25 μg/mL as-syn TiO_2 nanoparticles. Circle indicates association of nanoparticle clusters close to bacteria. Scale bar = 1 μm.

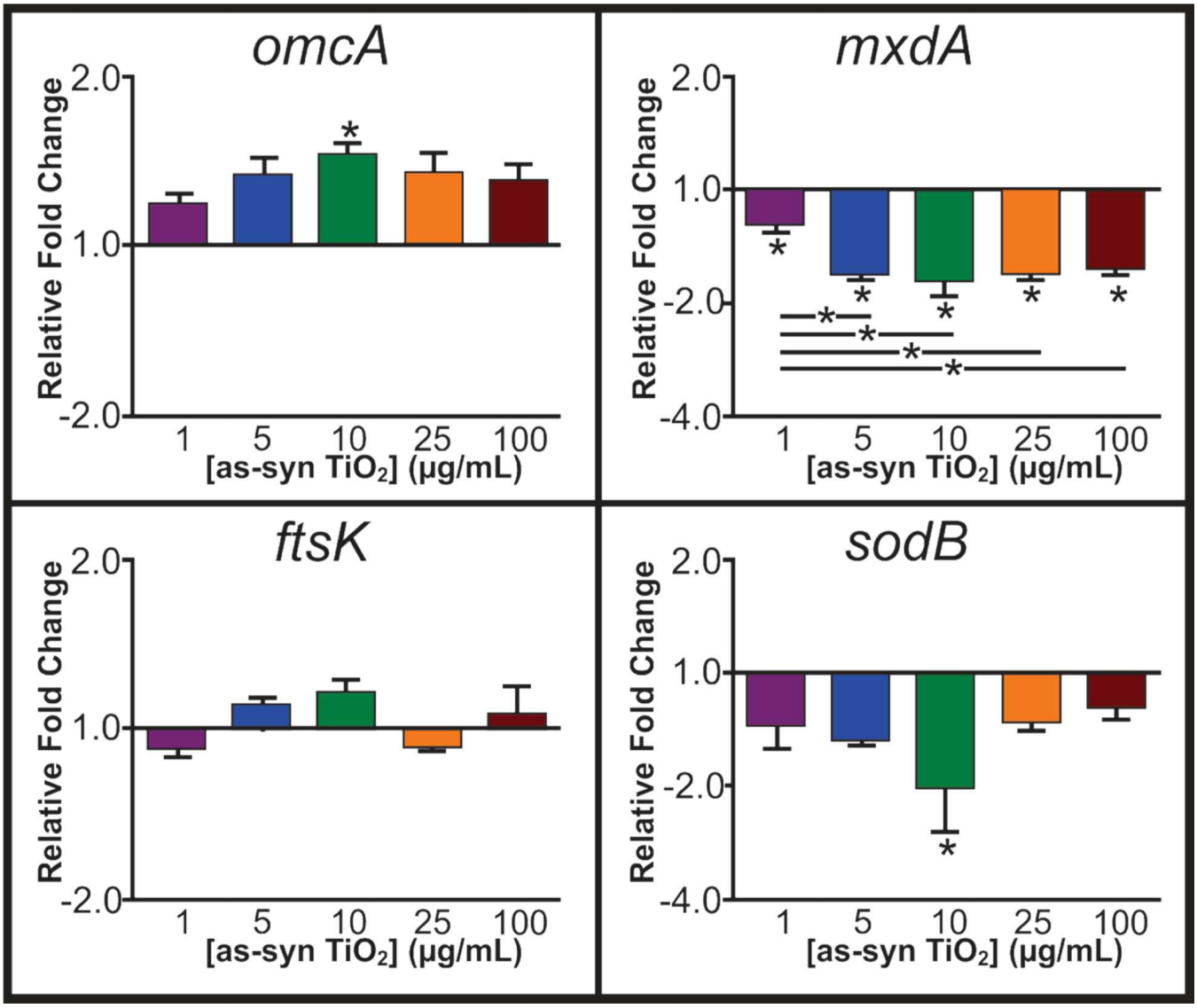

Figure 6.

Relative fold change of genes, as compared to a housekeeping gene, related to flavin secretion (*omcA*), biofilms/EPS (*mxdA*), growth (*ftsK*), and cell stress (*sodB*) upon 24 h exposure to varying concentrations of as-syn TiO_2 nanoparticles (*$p<0.05$).

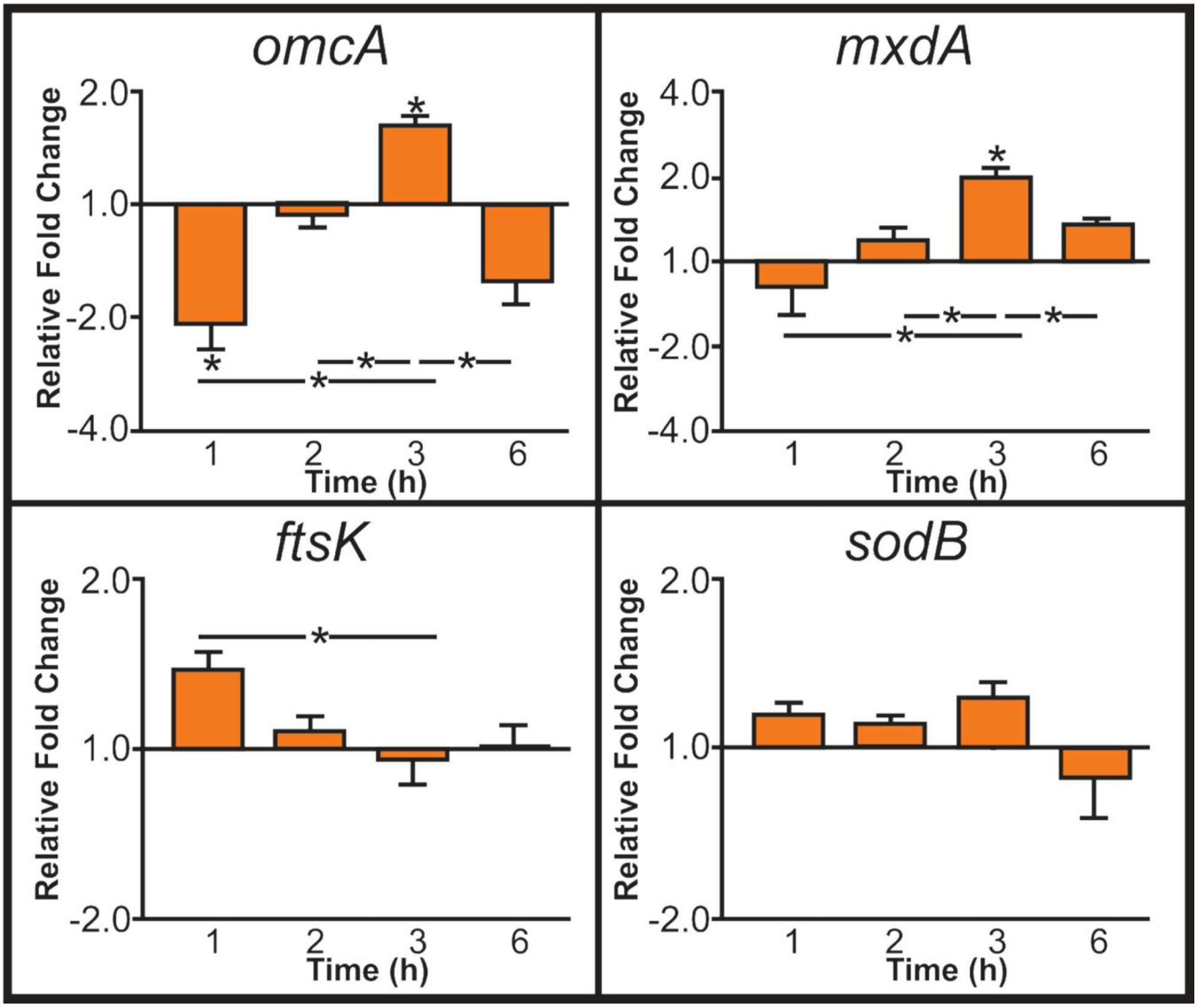

Figure 7.
Relative fold change of genes, as compared to a housekeeping gene, upon exposure to 25 μg/mL as-syn TiO_2 at varying times (*$p<0.05$).